VALIDATION OF A 3D MULTIPHASE-MULTICOMPONENT CFD MODEL FOR ACCIDENTAL LIQUID AND GASEOUS HYDROGEN RELEASES

Jäkel, C.[1], Kelm, S.[1] , Verfondern K.[1] and Allelein, H.-J.[2]

[1]Forschungszentrum Jülich, IEK-6, Jülich, 52425, Germany, [2]RWTH Aachen, LRST, Kackertstraße 9, Aachen, 52072, Germany

corresponding author: mail@christianjaekel.com

ABSTRACT

As hydrogen-air mixtures are flammable in a wide range of concentrations and the minimum ignition energy is low compared to hydrocarbon fuels, the safe handling of hydrogen is of utmost importance. Additional hazards may arise with the inadvertent spill of liquid hydrogen. An accidental release of LH2 leads to a formation of a cryogenic pool, a dynamic vaporization process, and consequently a dispersion of gaseous hydrogen into the environment. Several LH2 release experiments as well as modeling approaches address this phenomenology. Different model approaches have been validated in the past against the existing experimental data. These models can be divided into two sections:

1. Models calculating cryogenic pool propagation and vaporization rates,
2. Models calculating gaseous hydrogen dispersion using pre-calculated evaporation rates and pool surface areas as source term.

This leads to uncertainties if LH2 pool models lack relevant processes for vaporization, and in the gas distribution models the source term represents only an approximation of the real source term. At Forschungszentrum Jülich, a transient 3D multicomponent-multiphase model has been developed, using the commercial code ANSYS CFX 15.0 and including the additional sub-models of the rates of vaporization on solid ground, volume vaporization, humidity, and the influence of changing wind conditions. This new modeling approach is capable to simulate the release of LH2, its spreading and vaporization, and the gas distribution in the atmosphere under realistic environmental conditions (e.g. humidity and changing wind conditions). The model has been validated against recent LH2 spill experiments conducted by HSL and the NASA.

1.0 INTRODUCTION

The decarbonization of energy production, as a consequence of the global warming, has already started in leading industries, such as the automotive or the energy industry. Disruptive technology changes may support this process. One option towards a decarbonized environment are hydrogen-based technologies. Basically, the hydrogen supply can be set up quite similar to the todays supply of carbon based fuels. Gaseous high pressurized hydrogen (GH2) can be supplied via gas pipelines or discontinuously e.g. in tanks. Due to its high energy density, supply of liquid hydrogen (LH2) can be considered as economically valuable.

The prediction of the distribution of accidental released liquid hydrogen, its vaporization and consequently the distribution of an explosive gas cloud has been a reseach topic since many years. In former model approaches, the prediction of a release is separated into two parts:

1. Distribution of liquid hydrogen using a vaporization model and
2. Distribution of gaseous hydrogen using a source model.

The release and distribution models for the distribution of liquid hydrogen, the vaporization and the gaseous distribution can be separated into three sections:

1. Integral models, like GASP (Webber et al. [1], Batt et al. [2]),
2. Shallow-layer-models, like LAuV (Dienhardt and Verfondern [3, 4, 5]), and
3. Models on the basis of computational fluid dynamics (CFD), like CHAMPAGNE (Morii et al, [6], Chitose et al. [7]), ADREA-HF (Statharas et al., [8],Venetsanos et al. [9], Gianassi et al. [10, 11]), FLACS (FLACS, [12],Middha et al. [13], Ichard et al. [14]), and the commercial ANSYS FLUENT and CFX Codes (Schmidt et al., [15], Molkov et al., [16], Sklavounos et al., [17], Jäkel et al. [18]).

Most of the former cited CFD calculations calculate the gaseous distribution and Schmidt et al. [15] already stated in his analysis that a main difference between experiment and calculation is the assumption of the gas source. A CFD model which is capable of calculating liquid and gaseous phases is expected to be beneficial for accuracy and comprehension. The steps to achieve these goals are:

1. Identifying the physical phenomena for the distribution of e.g. the liquid phase (vaporization) and implementing a submodel to a CFD code.
2. Systematic validation using the existing experiments.
3. Discussion of limits and application range of the modeling approach.

A highly scalable and geometrical resolved 3D multicomponent-multiphase distribution model is considered to understand the phenomena and influences during the spill of liquid hydrogen. Consequently, it should allow to improve and substantiate reduced-order models.

2.0 EXPERIMENTS

The experimental procedure of available spill tests is comparable. At a time $t = 0s$ the cryogenic liquid is released. Depending on the release height, direction and momentum the liquid hydrogen propagates until a certain limit, where the,integral vaporization rate is equal to the inlet mass flow. In contact with the surrounding air and the ground the liquid starts to vaporize and the cryogenic vapor distributes according to several momentum sources such as e.g. wind, buoyancy and diffusion.

Release experiments of liquid hydrogen were conducted by the NASA (1980) [19, 20, 21], the BAM (1994) [3, 4], the HSL (2010) [22, 23] and most recently by Kawasaki Heavy Industries (2015) [24]. Within this paper only the NASA and the HSL experiments have been used for validation purpose, because the BAM release has been conducted on water and the Kawasaki test publication does not provide all necessary experimental data. The release experiments of the HSL (Health and Safety Laboratory) have been performed at Frith Valley, Buxton UK in 2010. The experiments have been conducted on a concrete pad with an radius of 16 m. During the test following sensors have recorded time series:

- one wind velocity and direction sensor in a height of 2 m at the release point,
- 24 ground thermocouples (GTC), arranged in release direction (or wind direction) to measure the pool propagation and
- 30 air thermocoupleas (ATC), beside TEST 10 arranged in wind direction.

Unfortunately the position and arrangement of the ATC towers are not completely available in open literature. Some of the distances, which could not be found in the official documentation, have been extracted from the available pictures (e.g. cf. Figure 1) and have been confirmed by HSL [25].

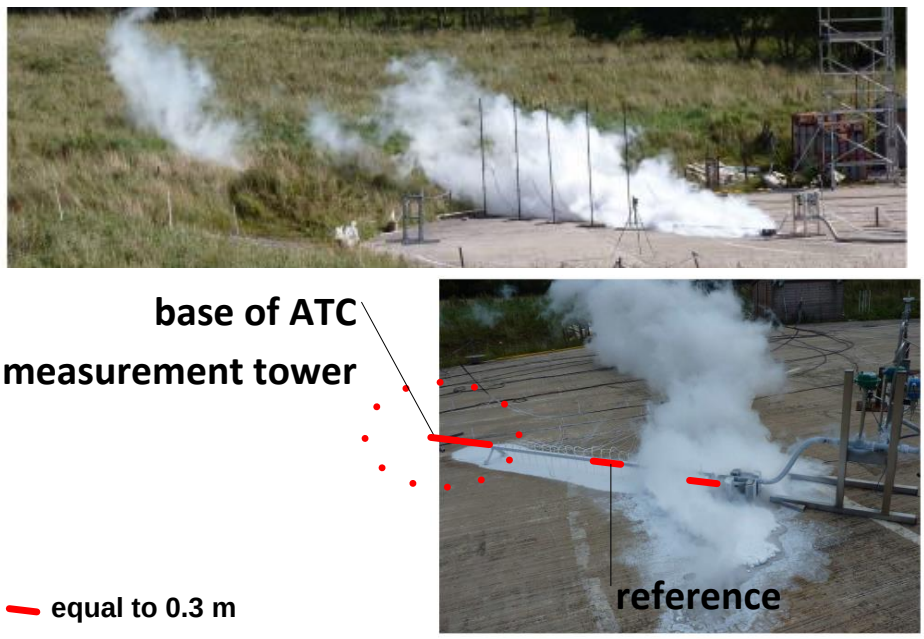

Figure 1: Pictures taken during TEST 06

The measurement density for the older NASA experiments (1980) is higher than for the HSL experiments, there is only a very small amount of data available, which is mainly documented in [19, 20, 21].

Table 1: Overview over the experiments

Test	**release height**	**release direction**	**duration in [s]**
HSL05	on ground	horizontal	248
HSL06	100 mm over ground	vertical downwards	561
HSL07	860 mm over ground	horizontal	305
HSL10	100 mm over ground	vertical downwards	215
NASA 06	100 mm over ground	vertical downwards	38

The principal arrangement of the HSL tests can be found in Figure 2a - c, the NASA experiment in Figure 2d. Table 1 gives an overview about release height, direction and duration of the experiments. Figure 2 illustrates these data and gives an overview of positions of the sensors, the wind and release direction.

For the HSL tests the wind data have been further analyzed and for each test a statistical analysis of the wind data, which resulted in a histogram pie chart, or wind rose (cf. Figure 3 for HSL TEST 05) has been conducted to identify stability criteria of the wind, as well as mean values for wind speed, wind direction and fluctuations.

All available data have been analyzed and following uncertainties of the experimental data have been identified:

- The geometrical position of the HSL sensors can not be determined exactly.

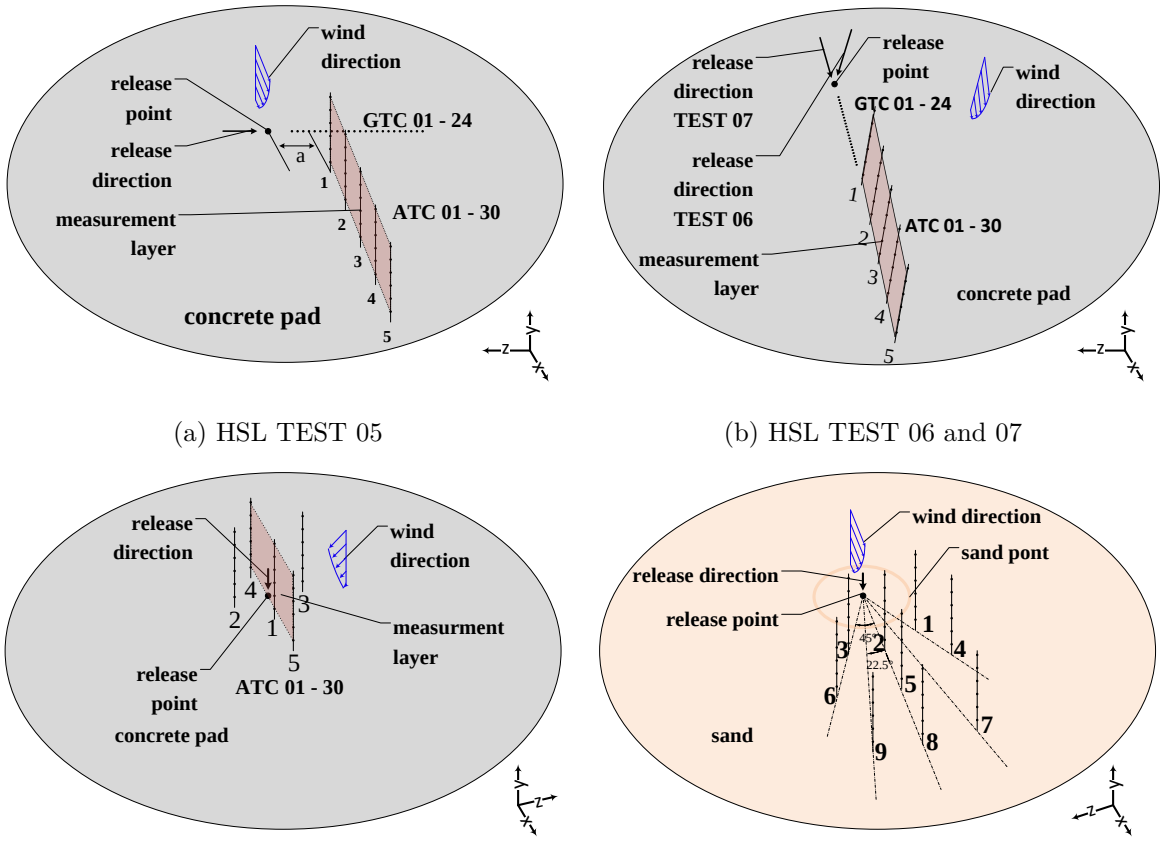

(a) HSL TEST 05

(b) HSL TEST 06 and 07

(c) HSL TEST 10

(d) NASA Test 06

Figure 2: Sketch of the thermoelements of the experiments - not drawn to scale

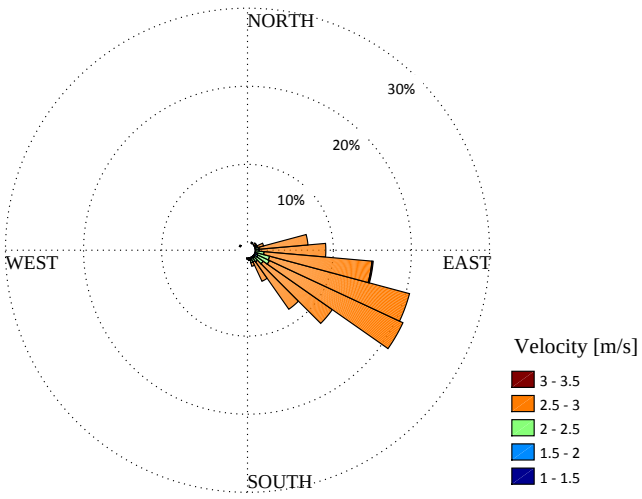

Figure 3: Histogram pie chart or wind rose of HSL TEST05

- The wind data of the HSL experiments is only measured at one point and the influence of the surrounded environment is not documented.
- A change of the wind direction during the release time can not be completely excluded; the statistics calculated for the whole duration may not reflect situations which occur at smaller time

spans.

- The low amount of data of the NASA experiment complicates validation.
- The measurement error and uncertainty is not documented for both experiments.
- The material properties of the ground is not fully clarified.

3.0 MODELING APPROACH

3.1 Conservation equations

The universally valid conservation equations for mass (IPCE - individual phase continuity), momentum (IPME - individual phase momentum equation) and energy (IPEE - individual phase energy equation) for an individual phase in a multiphase calculation are defined according to Brennen [26] to

$$\frac{\partial \rho_N}{\partial t} + \frac{\partial}{\partial x_i}\left[\rho_N u_{Ni}\right] = \xi_N, \quad i,j = 1,2,3 \tag{1}$$

$$\rho_N \alpha_N \left\{ \frac{\partial u_{N,i}}{\partial t} + u_{N,i}\frac{\partial u_{N,j}}{\partial x_i} \right\} = \alpha_N \rho_N g_i + F_{N,i} - \psi_N u_{N,i} - \delta_N \left\{ \frac{\partial p}{\partial x_j} - \frac{\partial \tau_{N,ji}}{\partial x_i} \right\} \tag{2}$$

$$\frac{\partial}{\partial t}\left(\rho_N \alpha_N e_{N,0}\right) + \frac{\partial}{\partial x_j}\left(\rho_N \alpha_N u_{N,j} e_{N,0}\right) + u_{N,j}p + q_{N,j} - u_{N,i}\tau_{N,ij} = Q\zeta_N + W\zeta_N \tag{3}$$

for a phase N. The term $F_{N,i}$ are external forces on the fluid and $Q\zeta_N + W\zeta_N$ are heat and mechanical work done on the fluid.

All conservation equations contain an interaction term, namely ξ_N for mass interaction, ψ_N for momentum interaction and ζ_N for energy interaction between the phases. In a two phase system with e.g. a liquid hydrogen phase $LH2$ and a gaseous phase $GH2$ these interaction terms can be definded as

$$\begin{aligned} \xi_{LH2} &= -\xi_{GH2} \\ \psi_{LH2} &= -\psi_{GH2} \\ \zeta_{LH2} &= -\zeta_{GH2} \end{aligned} \tag{4}$$

The interaction term ψ_N in the IPME (cf. Eq. 2) and the term $W\zeta_N$ in the IPEE (cf. Eq. 3) has been neglected for the used distribution model.

Consequently the mass interaction term has been defined to

$$\xi_{LH2} = \dot{m}_{vap} = \dot{m}_{vap,Wall} + \dot{m}_{vap,Vol} \tag{5}$$

the energy interaction term to

$$\zeta_{LH2} Q = \dot{q} = \dot{m}_{vap} \Delta h_{LH2 \rightarrow GH2,e} \tag{6}$$

with the term $\dot{m}_{vap,Wall}$ as the wall vaporization, $\dot{m}_{vap,Vol}$ as the volume vaporization, $\dot{q}$ the heat flux and $\Delta h_{LH2 \rightarrow GH2,e}$ the effective vaporization enthalpy. To implement wall vaporization, the heat flux density is determined for film boiling using the equation of Breen and Westwater, for the transition zone the equation of Zuber and for the nucleate boiling zone the equation of Kutateladze (cf. Figure

4, for more details please refer to Jäkel et al.[18] and Brentari et al.[27]). With the known heat flux density the mass flux density can be determined.

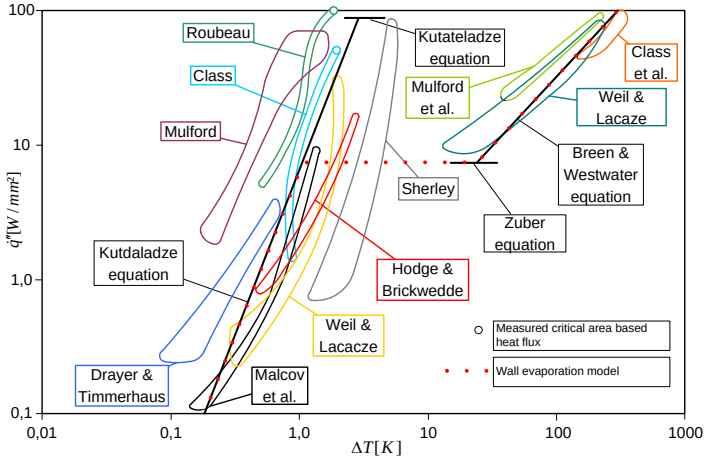

Figure 4: Nukiyama diagramm of liquid hydrogen, comparison of different experimental results and analytical equations for calculating the heat transfer according to Brentari et al. [27]

The volume vaporization uses a homogeneous equilibrium approach, which is widely used in industrial applications. For this approach the saturated vapor line for hydrogen is needed, which is obtained from the NIST database [28]. With this curve, based on the knowledge of pressure and temperature, a mass flux density can be determined for every mesh cell to

$$\dot{m}'''_{vap,Vol} = \dot{M}\,(x - x_{quota,GH2}) \tag{7}$$

with $\dot{M}$ as a numerical stabilization equation and x as the local volume fraction. The quota volume fraction is determined based on pressure and temperature in a discrete finite volume cell according to

$$x_{quota,GH2} = \frac{p_{sat}}{p_{absolute}} \frac{M_{GH2}}{M_{mixture}} \tag{8}$$

with M_{GH2} and $M_{mixture}$ as the molar mass of gaseous hydrogen and the gas mixture. In analogy to this, vapor condensation in humid air has also been modeled. The saturated vapor lines for water and hydrogen, which have been used in this model, are displayed in Figure 5.

3.2 Boundary conditions

A generic overview of the boundary conditions can be found in Table 2. During the model development and the detailed analysis of the experimental data the importance of the wind has been identified and needed to be considered in an atmospheric flow model.

The demand of most realistic boundary condition of the atmospheric flow leads to model based on the Pasquill stability criterion. According to Mannan et al.[29] the velocity profile normal to the ground can be defined according to

$$\vec{u}_x = \vec{u}_r \left[\frac{x_1}{x_r}\right]^{2*f_{Pasquill}} R(t) \tag{9}$$

with a reference velocity u_r at a reference height x_r. The exponent $2 * f_{Pasquill}$ needs to be chosen according to the stability of the wind. It needs to be distinguished between stable, neutral and unstable wind conditions. This conditions have been accounted by using a random function $R(t)$, which has been

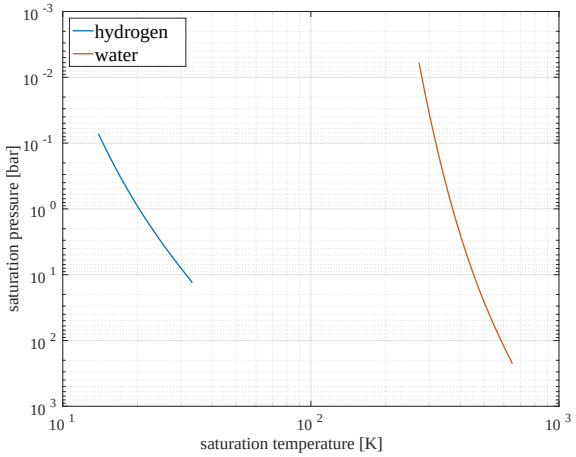

Figure 5: Logarithmic plot of the function $p_s = f(T_s)$ for hydrogen and water vapor

Table 2: Generic boundary contitions

boundary conditions	Option
Inlet	wind conditions according to experimental set up; constant air temperature and humidity
Outlet	static pressure $P = 0Pa$
Inlet Hydrogen	LH2/GH2- mass flow, condition based on flash vaporization at inlet
Wall, ground	no slip adiabatic (in case no contact to LH2) source/sink (cf. Eq. 5, 6 in case of contact with LH2)
further source/sink	H2O condensation (single phase model)

determined once and used within every calculation. Furthermore, the azimuthal and the vertical velocity component of the wind can be determined using the normal velocity profile and the Pasquill stability criterion by using

$$\pm\vec{u}_y = \vec{u}_x f_{Pasquill,azimuthal} R(t) \tag{10}$$

and

$$\vec{u}_z = \vec{u}_x f_{Pasquill,vertical} R(t) \ . \tag{11}$$

The factors $f_{Pasquill,azimuthal}$ and $f_{Pasquill,vertical}$ have also be taken from Mannan et al.[29].

3.3 Grid, initial and boundary conditions

Table 3 contains the initial conditions at the hydrogen inlet. Due to the depressuriation at the inlet a certain amount of hydrogen is released already as saturated vapor. This amount can be determined using the T-s diagram of hydrogen, which is also provided by NIST [28].

Figure 6 and 7 are showing the geometrical models, at some of the boundaries the grid vertical is displayed. The quality values for the different meshs can be found in Table 4 and fulfil the common Best Practice Guidelines (BPG) requirements, taken from Menter et al. [30], Mahaffy et al. [31] or ANSYS [32]. The grid convergence index for HSL TEST05 indicates that for this calculation a grid

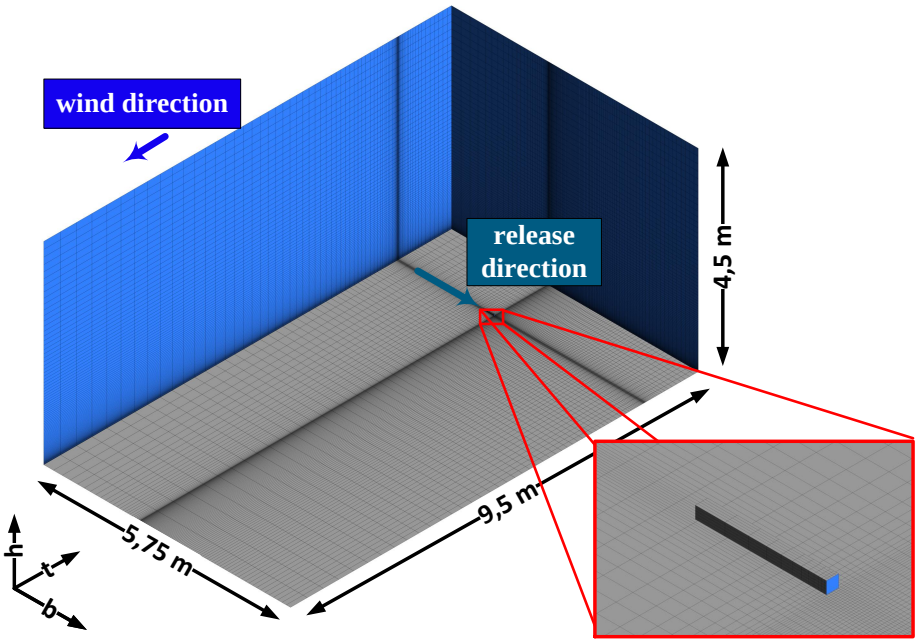

Figure 6: Geometrical model HSL TEST 05 incl. enlargement of the hydrogen inlet, as well as wind and release direction

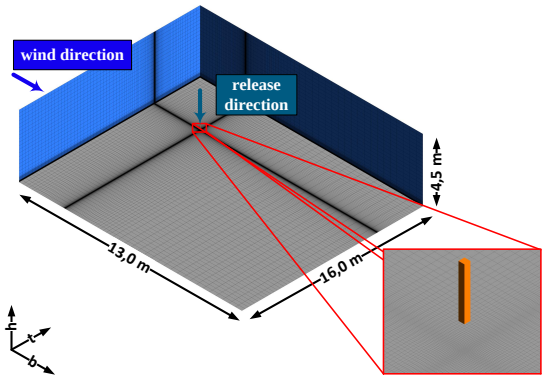

(a) TEST 06

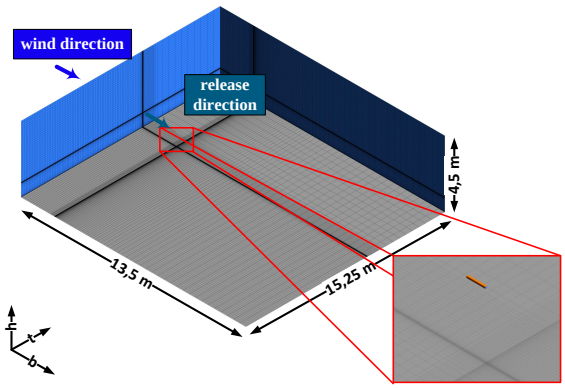

(b) TEST 07

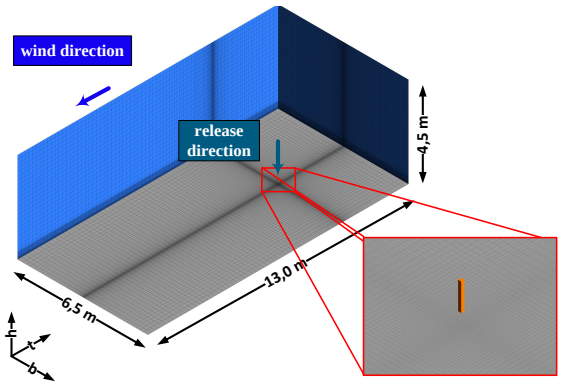

(c) TEST 10

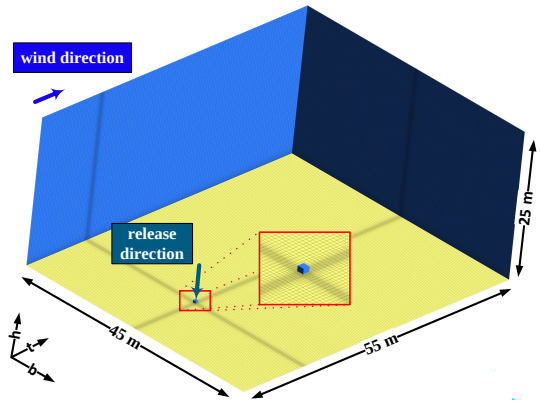

(d) NASA T06

Figure 7: Geometrical model incl. enlargement of the hydrogen inlet, as well as wind and release direction

independence study has been successfully performed. These values indicate that the numerical errors

Table 3: Test parameters [22]

experiment	**release rate [l/min]**	**LH2/GH2 at inlet [Vol.-%]**
HSL	60	93.7/6.3
NASA	8100	66/33

related to spatial discretization have been minimized. Consequently it is expected, that the differences, which will be found in the results in comparison to the experimental results are model errors and experimental measurement uncertainties.

Table 4: Characteristic values of grid quality, according to Menter et al. [30], Mahaffy et al. [31] and GCI according to Celik [33]

TEST	HSL05	HSL06	HSL07	HSL10	NASA	BPG
number of elements [Mio]	1.4	1.2	1.3	1.4	2.0	
volume grow rate [-]	4.94	2.6	5.5	2.4	2.44	< 8
angle [°]	85.5	89.28	87.03	89.28	89.91	> 20
aspect ratio [-]	73.58	94.53	184.20	94.12	13.63	< 100
grid convergence index (GCI)	< 3 %					

4.0 RESULTS

4.1 Pool propagation

HSL TEST 05 asymmetric pool spreading has not yet been calculated by existing models. Consequently there is no possibility of code to code benchmarking the results. Only the comparison against the available experimental data (Thermocouples) is possible.

There are calculations of the axis-symetric pool distribution of Batt et al.[2] of HSL TEST 06 using GASP (an integral code, for further information see [1]), and for the NASA Test 06 of Dienhart[3, 4] using LAuV (a shallow layer code, developed at Forschungszentrum Jülich) and by Middha et al. [13] using FLACS (a 3D CFD Code).

Figure 8 shows the comparison of the experimental results, the calculation results and the calculation results of the HSL TEST 05 and 06, Figure 9 of the NASA experiment. To obtain the experimental results from the HSL experiments two different methods have been applied, which are in accordance for HSL TEST 06 with the results of Batt et al. [2]. For the HSL experiments the formerly mentioned GTC measurements are available as time series. From the data it can be taken both, the position and the time, when the temperature of the thermocouple falls below a certain temperature limit (here $T_{lim} = 50K$) and when the highest temperature gradient occurs. Both informations are expected to provide the pool front. For the calculation the pool front is expected to be at a volume fraction of $x_{LH2} = 0.5$. The volume fraction of $x_{LH2} = 0.1$ is also plotted, give an indication about the spread of the transition area between liquid and gaseous phase.

Considering Figure 8a and b, the results for the HSL experiment are qualitatively consistent with the experimental data. The backstepping in Figure 8b is caused by the method used for analyzing the experimental data. Every cross is equal to a ground thermocouple and it is tracked when the ground thermocouples has reached 50 K for the first time (Batt et al. [2]). In the experiments the occurrence of slush air (N2/O2) has been observed, but is not considered in this model. That implies that at roughly 50 K a plateau can be seen in the experimental data, which is a strong hint to the occurrence of slush air. The thermocouples GTC07 falls below the limit of 50 K 4s before thermocouple GTC06. For the NASA test (cf. Figure 9), the pool size is systematically overestimated by the CFD model and the other bench-marked codes. This overestimation has been explained by Dienhart as an uncertainty

of the ground properties. The hydrogen has been released on sand, the porosity and the humidity of the sand has not been provided. In the calculation they had been considered as hydraulically smooth with dry sand properties. To account for the corrugation and the porosity of the sand surface, the CFD model uses an additional factor for the wall vaporization rate of 50 %. Even this additional increasing factor only brings the pool in the size of the experimental results.

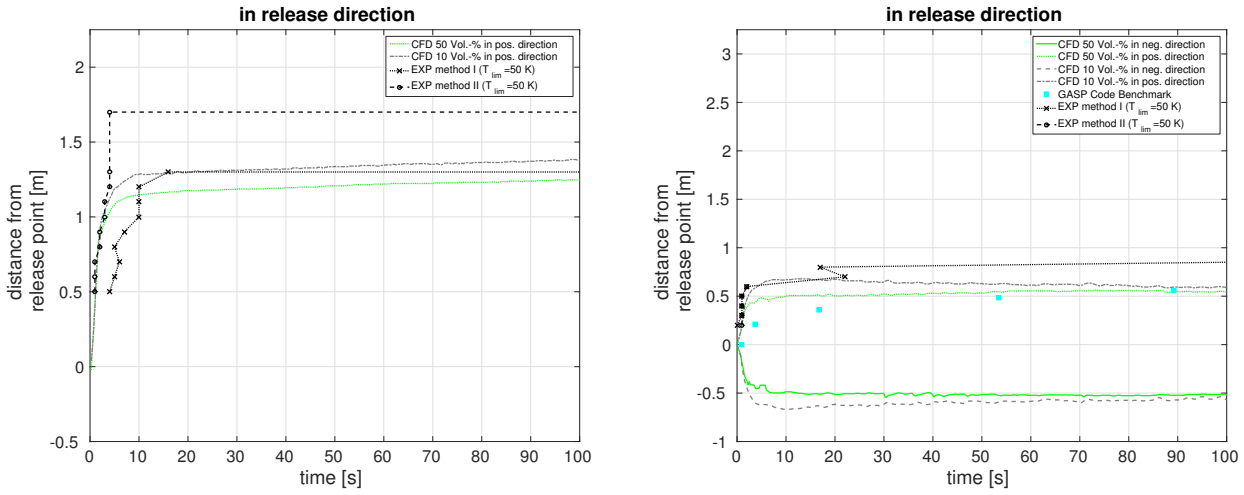

(a) HSL TEST 05

(b) HSL TEST 06

Figure 8: Size of pool, determined from the CFD results by the volume fraction $x_{LH2} = 0.5$, benchmarked with GASP for HSL TEST 06

To provide some more details of the pool size, an isosurface with the volume fraction of $x_{LH2} = 0.5$ for different time steps has been taken from the calculation and is displayed within Figure 10. The plots include the measurement position of the sensors, for the NASA test there are more sensors displayed than used during the test. Furthermore, the ATC positions and the measurement towers are displayed.

The available experimental data do not allow to directly validate the calculated integral vaporization rate. Figure 9b gives the indication that the available codes predict the vaporization rate for the NASA test in the same range.

Anyway the pool size is implicitly determined from the thermocouple measurement, with the consequent uncertainties. The sparse information from the experiments makes more detailled validation difficult, also a validation of the different sub-models such as the vaporization rate is not possible. Nevertheless the results are quantitatively consistent. Qualitative deviations, which have been found during the validation process, are within the experimental uncertainties.

The relative good agreement with both the experimental data (HSL) and the benchmark results the pool distribution of the multiphase-multicomponent developed model leads to the conclusion that in accordance with the uncertainty of the experimental data the results are taken as quantitatively validated. Regardless, further validation effort needs to be made and new experimental data should be used for further validation of the model.

4.2 Gas distribution

As already mentioned in section 2.0 the cloud distribution for the HSL tests has been measured by 30 air thermocouples (ATC). The ATCs are arranged in wind direction and span a measurement layer. For all tests this data is used for further validation. The ATCs' qualitative positions can be found in Figure 2a.

This measurement plane can also be extracted from the calculation. Figure 11 shows two different contour plots. For the contour plot in Figure 11a the data from Figure 11b is taken and analyzed. The

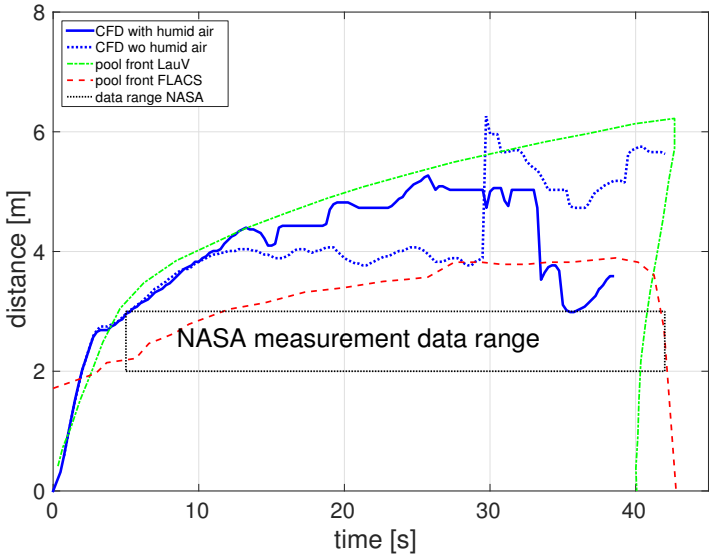

(a) NASA

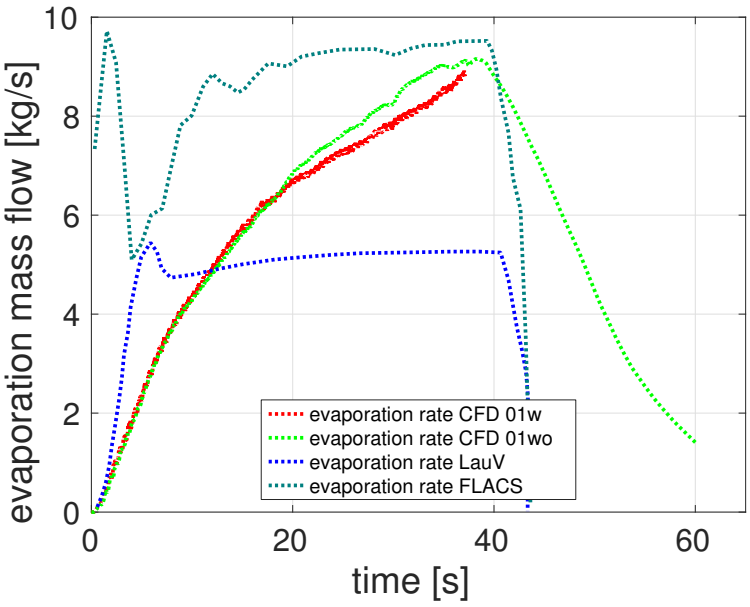

(b) calculated NASA vaporization rates

Figure 9: Size of pool of the NASA calculation, determined from the CFD results by the volume fraction $x_{LH2} = 0.5$, benchmarked with FLACS ([13]) and LauV ([4, 3])

aim of this pre-analysis is to obtain further information from the contour plot, such as the distribution vector (cf. in Figure 11a lower left corner) of the gas cloud. The data was taken from the results and was cut at the distances of the first and last ATC towers. Using the local minima a distribution vector has been obtained from this data.

Figure 12 shows the results at $t = 40s$ of the HSL TEST 05 calculation. In this figure the gas cloud is displayed as an isosurface using the lower flammability limit (LFL) of 4 Vol.-%. Furthermore, the ATC measurement towers are displayed, which are arranged in wind direction and normal to the wind direction through the towers additional temperature contours plots are drawn. From this plot a 3D dependency of the gas cloud on the wind direction can be clearly identified. From this plot it can be found, that for the validation not the "best" measurement plane is spanned by the towers. The towers just detect one side of the cloud. Unfortunately, the distance a (between release point and first tower normal to the wind direction, which is equal to release direction) in Figure 2a, is not documented and has been assumed by using the pictures of the experiment, such as Figure 1, in this calculation being 1.5

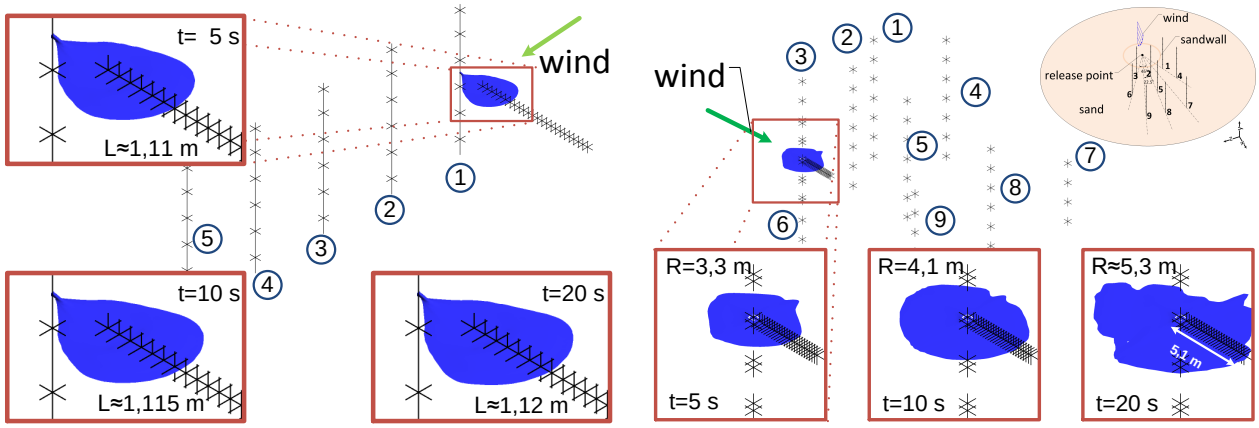

(a) HSL TEST 05 (b) NASA

Figure 10: Pool distribution for different time steps

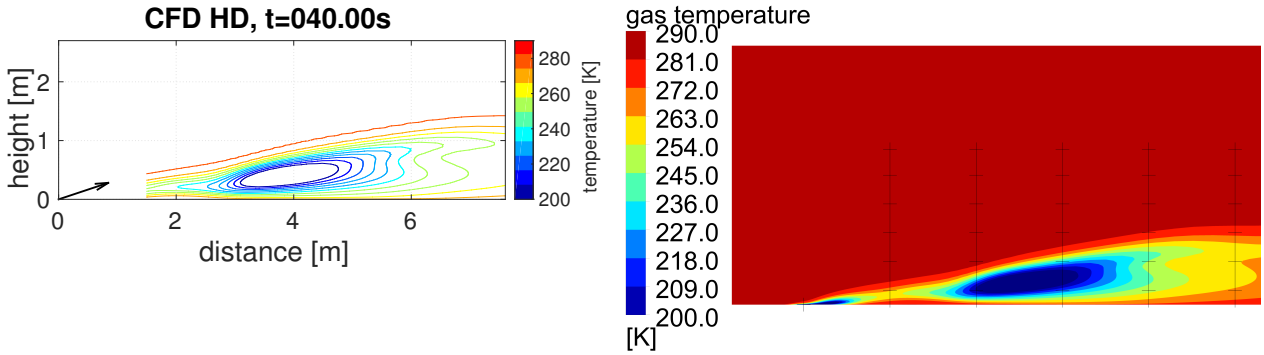

(a) CFD 40,00 s, measurement plane (b) CFD 40,00 s, complete plane incl. hydrogen inlet

Figure 11: Iso-temperature plot of the CFD results, HSL TEST 05

m. Due to this uncertainty only a qualitative consistency can be concluded.

With the spatial information and the time series of the sensors the experimental data can be further analyzed and an iso-temperature plot similar to the calculation results can be obtained. This plot can be seen in Figure 13a for the time $t = 40s$. The data between the measurement points have been interpolated and an iso-temperature contour plot has been drawn. This figure contains several additional information from the experimental data, which can not be seen by simply using the individual sensor time series. It looks like that between 1.5 m (Tower 1) and 3.0 m (Tower 2) at a height between 0.25 and 1.25 m the gas cloud, as well as at a distance between 6.0 and 7.5 m from the release point another low temperature region can be detected. The certainty that this is the hydrogen cloud is high. With this data also a distribution vector can be drawn, which can also been found in the plot. There is an immense reduction in resolution from mesh density in Figure 11 to 30 supporting points in Figure 13a. Some of the information will be lost due to the lack of supporting points.

Therefore, Figure 13b shows the results of the calculation at the same time $t = 40s$ with the same amount of supporting points at the same spatial position determined from the calculation results. This time step can be used as the proof of quantitatively agreement between experimental results and calculation data.

The vector in 13a, b and 11a has been determined from the data by identifying the local minima of the temperature and fitting a line through the minima positions and the origin for every time step. The

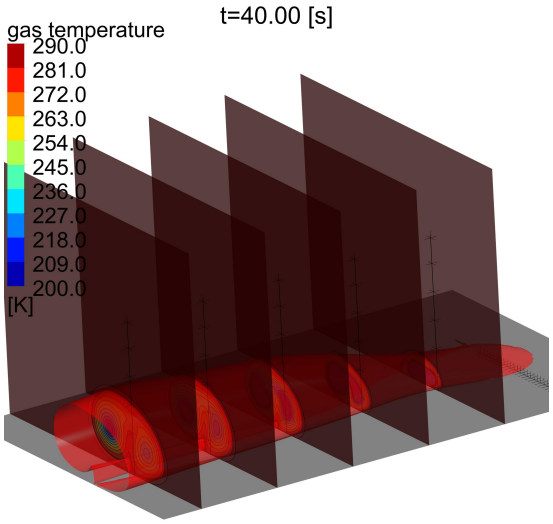

Figure 12: Iso-temperature plots normal to the wind direction at different distances (the distances of the ATC measurment towers) and the isosurface of the 4 Vol.-% LFL limit of the hydrogen-air cloud of HSL TEST 05

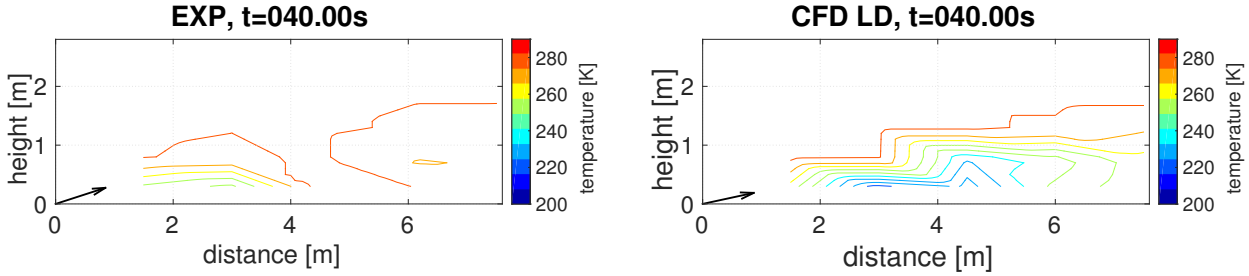

(a) EXP 40,00 s

(b) CFD LD 40,00 s

Figure 13: Iso-temperature plot of the experiment (EXP) and the CFD results, determined with the same resolution as the experiments, HSL TEST 05

mean distribution vector (determined by using all available time steps) for the TEST05 until TEST07 can be found for the experiment, the results using the same resolution as the experiment and the mesh resolution of the calculation results can be found in Figure 14.

For TEST 05 the conformity of the distribution vectors between experiment and calculation is quantitatively good. Between the vectors of TEST 06 and TEST 07 the experimental data shows a higher buoyancy of the gas cloud than the vectors from the calculation. If the experimental data and the calculation data is further analyzed, it becomes clear that the distribution vector of the calculation is clearly affected by the low temperatures of the gas just vaporized. This low temperatures can not be found in the experimental data. The ATC 10, which is located at Tower 1 at a height of 0.25 m for TEST 06 and TEST 07 only measuring the lowest temperature of 225 K, but 150 K are calculated in the first 100 s.

Again, it is questionable whether the cloud is completely detected from the ATC measurements. The cloud is clearly affected by the wind field, which can hardly represented by the calculation. This observation is supported if e.g. the Figure 1, which is taken during TEST 06, is further analyzed. The

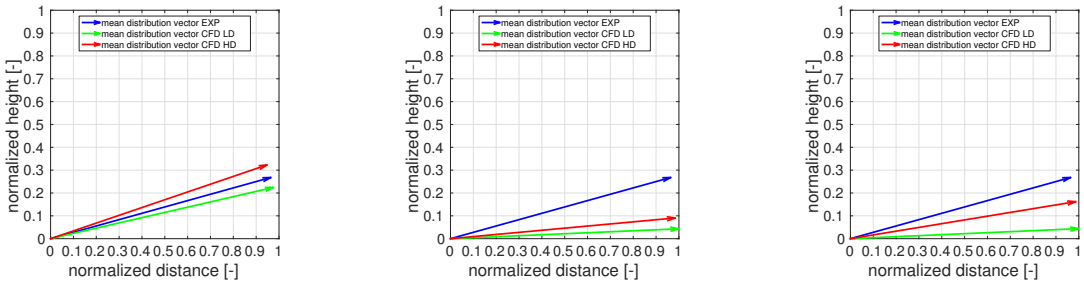

(a) HSL TEST 05 (b) HSL TEST 06 (c) HSL TEST 07

Figure 14: Visualisation and comparision of the different distribution vectors obtained from experiment and the calculation with 30 supporting points (CFD LD) and mesh resolution (CFD HD)

upper figure shows a visible cloud and the tower, which can be found in the picture, does not seem to be within the cloud, but in front of it.

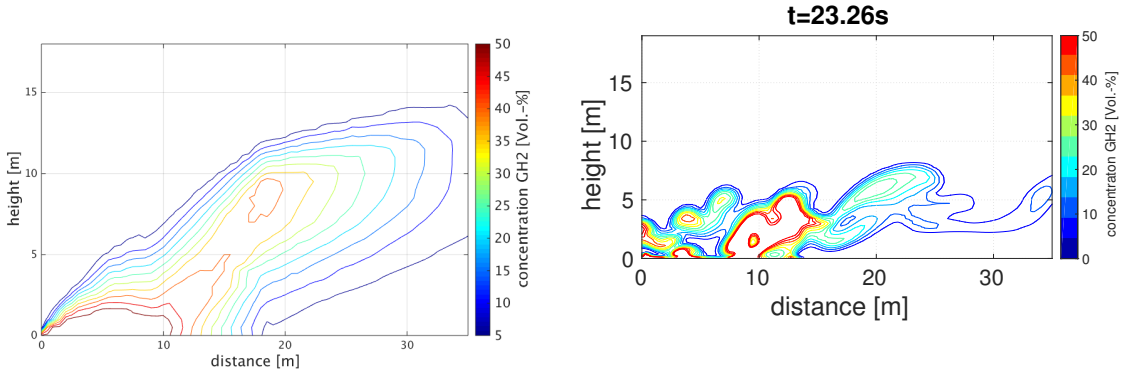

(a) Experiment $t = 21,33\ s$ (b) Concentration

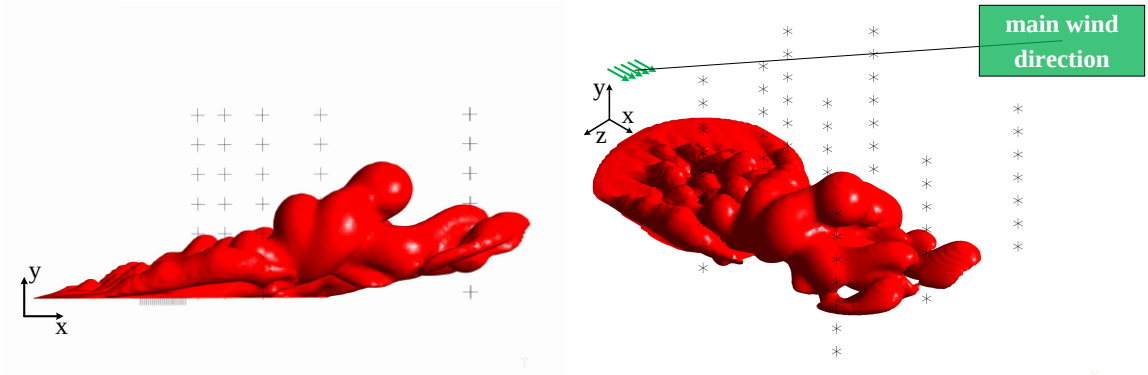

(c) Side view, /wo humid air (d) Isometric view, /wo humid air

Figure 15: Comparision of the concentration contour plots of experiment and calculation and isosurface of the hydrogen cloud at LFL limit in the side and isometric view of the NASA TEST 06

With the identified uncertainties of the experimental boundary conditions and the comparison of calculational and experimental data, the HSL gas distribution leads to the conclusion, that the developed model predicts a reasonable and qualitatively consistent distribution. Given the fact that no detailed measurement of the gas composites is available. The model is considered as valid, however it needs to be further assessed when newer, more complete (that provide not just temperature measurements) data sets are available.

Furthermore, the NASA experiment has been calculated with the same model and generic boundary

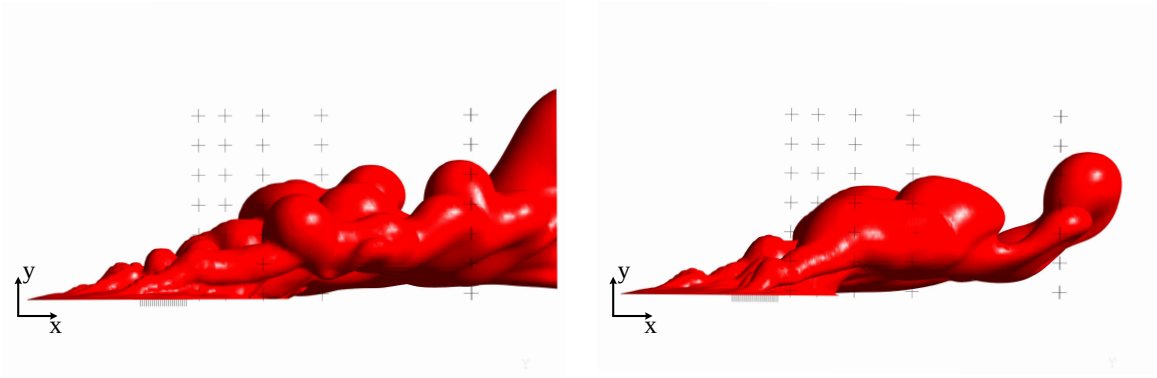

(a) Calculation side view /w humid air, $t = 29.25s$ (b) Calculation side view /wo humid air, $t = 29.25s$

Figure 16: Comparison of the 4 Vol.-% LFL limit - effect of humid air condensation on the gas cloud

conditions (e.g. the wind data has been taken from the documentation). The faces normal to the main wind direction have been set as symmetry planes, used in the HSL models at either in- or outlets. As already mentioned the available experimental data point are less than the data from the HSL experiments, nevertheless the identified uncertainties for the HSL experiments also apply for the NASA experiment. Figure 15 gives an overview of the experimental data (cf. Figure 15a) and the corresponding concentration plot through the same measurement plane in the calculation. In the gas distribution there have been significant differences between the calculation and the experimental data at the same time step for the same boundary conditions than in the HSL cases. The decision was made to change the normal to the wind faces to symmetry boundary conditions. The result can be seen in Figure 15b until d. Figure 15b shows the concentration plot through the same measurement plane than in Figure 15a. Figure 15c shows the side view of this time step and d the isometric view. Comparing the results a quantitatively agreement can be found.

The NASA test has been used to demonstrate the influence of the humid air model. The test has been calculated either with and without the humid air model. It has been found that the difference can be detected at later time step. The results can be found in Figure 16a for the case with humid air model and in b the case without humid air model. The differences between the cases are not significant, so far because there is a small indication that the buoyancy of the cloud is increased slightly (as expected) for the case with humid air.

For a further validation of this model additional experimental data is needed. Following information and restrictions are mandatory for a further validation:

1. The experimental releases should be done in more confined spaces to reduce the influence of the wind.
2. The ground needs to be analyzed and well prepared to decrease uncertainties.
3. Possible future experiments need to be equipped with more thermocouples at the ground and in the air, either for pool and gas propagation.
4. Further analysis methods for the temperature measurement need to be further discussed.

5.0 CONCLUSIONS

A multicomponent, multiphase CFD model has been developed to predict an accidental LH2 spill and resulting gas cloud propagation. A comprehensive validation was carried out for both gas and liquid distribution based on available data from HSL and NASA LH2 spill experiments. Qualitatively, no

systematic deviation between simulation, experimental data (and previous modeling results for axis-symmetric tests (for HSL TEST 06 GASP and NASA LauV, FLACS)) could be identified. However quantitatively, there are differences, which fall in the range of the experimental uncertainty: The tests main instrumentation are thermocouples in the ground and at towers around the release location. This information was applied to determine the arrival/presence of the cryogenic liquid and gas. Thus, the pool spreading and gas distribution could be assessed implicitly, however no direct measure e.g. of the vaporization rate or the gas concentrations is available, which could directly allow to substantiate or improve the sub models.

Considering the liquid spreading and vaporization, the model revealed to be in particular sensitive to the defined ground properties (heat capacity, thermal conductivity, porosity, roughness etc.), which are practically affected by a large uncertainty. The propagation of the formed cryogenic gas cloud is significantly influenced by the definition of the atmospheric boundary conditions (instantaneous 3D wind field, temperature, humidity etc.), which can hardly be quantified in an open environment to the necessary level of detail. On basis of these uncertainties and the qualitative consistency between simulation and experimental data, a first successful validation of the model can be concluded. However, further validation has to be carried out as soon as new experimental results are available. In this regard, measurements under simplified well defined boundary conditions, and capturing different quantities like, temperature, concentration, wall heat fluxes are necessary. In addition, a videometric evaluation may help to get further insight in the phenomenology.

As of now, the CFD modeling basis for predicting three dimensional LH2 spills and GH2 distribution is available and expected to provide a detailed insight into the phenomenology of accident scenarios at industrial scale. Even though the high computational effort practically prohibits its comprehensive application, the model can be applied in the frame of a safety assessment in order to analyze identified critical cases and to substantiate the results obtained by reduced order approaches.

Future modeling work will address the definition of the atmospheric and ground boundary conditions. The model will be applied to generic scenarios in order to demonstrate its capabilities and summarize experiences in a best practice guideline.

Further information and more details can be found in [34].

References

[1] D.M. Webber. *A model for pool spreading and vaporisation and its implementation in the computer code GASP*. Tech. rep. SRD / HSE / R521, 1990.

[2] R. Batt and D.M. Webber. *Modelling of liquid hydrogen spills, HSL report RR985*. Tech. rep. HSL, UK, 2012.

[3] B. Dienhart. *Ausbreitung und Verdampfung von flüssigen Wasserstoff auf Wasser und festem Untergrund, Berichte des Forschungszentrum Jülich, 3135*. Schriften des Forschungszentrum Jülich, 1995.

[4] K. Verfondern and B. Dienhart. "Experimental and theoretical investigation of liquid hydrogen pool spreading and vaporization". In: *International Journal of Hydrogen Energy* 22.7 (1997), pp. 649 –660.

[5] K. Verfondern and B. Dienhart. "Pool spreading and vaporization of liquid hydrogen". In: *International Journal of Hydrogen Energy* 32.2 (2007), pp. 256 –267.

[6] T. Morii and Y. Ogawa. "Development and application of a fully implicit fluid dynamics code for multiphase flow". In: *Nuclear Technology* 115.3 (1996), pp. 333–341.

[7] K. Chitose, Y Ogawa, and T. Morii. "Analysis of a large scale liquid hydrogen spill experiment using the multi-phase hydrodynamics analysis code." In: *Proceedings of the 11th World Hydrogen Energy Conference* (1996).

[8] J.C. Statharas, A.G. Venetsanos, J.G. Bartzis, J. Würtz, and U. Schmidtchen. "Analysis of data from spilling experiments performed with liquid hydrogen". In: *Journal of hazardous materials* 77.1 (2000), pp. 57–75.

[9] A.G. Venetsanos and J.G. Bartzis. "CFD modeling of large-scale LH2 spills in open environment". In: *International Journal of Hydrogen Energy* 32.13 (2007), pp. 2171–2177.

[10] S.G. Giannissi, A.G. Venetsanos, J.G. Bartzis, N. Markatos, D.B. Willoughby, and M.Royle. "CFD MODELING OF LH2 DISPERSION USING THE ADREA-HF CODE". In: *Proc. 4th Int. Conf. on Hydrogen Safety, September 12-14, San Francisco, CA* (2011).

[11] S.G. Giannissi, A.G. Venetsanos, N. Markatos, and J.G. Bartzis. "CFD modeling of hydrogen dispersion under cryogenic release conditions". In: *International Journal of Hydrogen Energy* 39.28 (2014), pp. 15851–15863.

[12] *FLACS v9.1 User's Manual*. GexCon AG. 2010.

[13] P. Middha, O. R. Hansen, and I. E. Storvik. "Validation of CFD-model for hydrogen dispersion". In: *Journal of Loss Prevention in the Process Industries* 22.6 (2009), pp. 1034 –1038.

[14] M. Ichard, O.R. Hansen, P. Middha, and D. Willoughby. "CFD computations of liquid hydrogen releases". In: *International Journal of Hydrogen Energy* 37.22 (2012), pp. 17380 –17389.

[15] D Schmidt, U Krause, and U Schmidtchen. "Numerical simulation of hydrogen gas releases between buildings". In: *International journal of hydrogen energy* 24.5 (1999), pp. 479–488.

[16] V.V. Molkov, D.V. Makarov, and E. Prost. "On numerical simulation of liquefied and gaseous hydrogen releases at large scales". In: *First International Conference on Hydrogen Safety, Pisa, Italy*. 2005, pp. 8–10.

[17] S. Sklavounos and F. Rigas. "Fuel Gas Dispersion under Cryogenic Release Conditions". In: *Energy & Fuels* 19.6 (2005), pp. 2535–2544. eprint: `http://pubs.acs.org/doi/pdf/10.1021/ef0500383`.

[18] C. Jäkel, K. Verfondern, S. Kelm, W. Jahn, and H.J. Allelein. "3D Modeling of the Different Boiling Regimes During Spill and Spreading of Liquid Hydrogen". In: *Energy Procedia* 29.0 (2012). WHEC 2012 Conference Proceedings, 19th World Hydrogen Energy Conference, pp. 244 –253.

[19] R. Witcofski. "Experimental Measurements of the dispersion of flammable clouds formed by liquid hydrogen spills". In: *1981 JANNAF Safety & environmental protection subcommittee meeting*. 1981.

[20] R.D. Witcofski and J.E. Chirivella. "Experimental and analytical analyses of the mechanisms governing the dispersion of flammable clouds formed by liquid hydrogen spills". In: *International Journal of Hydrogen Energy* 9.5 (1984), pp. 425 –435.

[21] J.E. Chirivella and R.D.Witcofski. *Experimental Results from fast 1500-Gallom LH2 Spills*. Tech. rep. NASA, 1986.

[22] D. Willoughby and M. Royle. *Release of unignited liquid hydrogen, HSL report RR986*. Tech. rep. HSL, UK, 2012.

[23] J. Hall. *Ignited release of liquid hydrogen, HSL RR987*. Tech. rep. HSL, UK, 2014.

[24] S. Unno, Y. Takaoka, S. Kamiya, S. Qyama, A. Kishimoto, Y. Miida, and H. Suga. "A study on dispersion resulting from liquefied hydrogen spilling". In: *Proceedings of the 6th International Conference on Hydrogen Safety*. 2015.

[25] J. Hall. "personal communication with Jonathan Hall, HSL, 10.07.2016".

[26] C.E. Brennen. *Fundamentals of Multiphase Flows*. California Institute of Technology, Pasadena, California, 2005.

[27] E.G. Brentari, P.J. Giarratano, and R.V. Smith. *Boiling Heat Transfer for Oxygen, Nitrogen, Hydrogen and Helium, Technical Note Nr. 317*. Tech. rep. US Departement of Commerce, National Buereau of Standards, 1965.

[28] National Institute of Standards. *Models and Tools: Thermophysical Properties of Fluid Systems; High accuracy data for a select group of fluids.* USA. 2011-2012. URL: `http://webbook.nist.gov/chemistry/fluid/`.

[29] S. Mannan. "15 - Emission and Dispersion". In: *Lees' Loss Prevention in the Process Industries (Third Edition)*. Third Edition. Burlington: Butterworth-Heinemann, 2005, pp. 1 –348.

[30] F. Menter et al. *CFD Best Practice Guidelines for CFD Code Validation for Reactor-Safety Applications*. Tech. rep. EUROPEAN COMMISSION, 5th EURATOM FRAMEWORK PROGRAMME, 2002.

[31] J. Mahaffy, B. Chung, C. Song, F. Dubois, E. Graffard, F. Ducros, M. Heitsch, M. Scheuerer, M. Henriksson, E. Komen, et al. *Best practice guidelines for the use of CFD in nuclear reactor safety applications*. Tech. rep. No. NEA-CSNI-R–2007-05; Organisation for Economic Co-Operation and Development, 2007.

[32] Ansys Inc. *Documentaion, Ansys Inc., Canonsburg*. 2012.

[33] I. B. Celik. "Procedure for Estimation and Reporting of Uncertainty Due to Discretization in CFD Applications". In: *Journal of Fluids Engineering* 130.7 (2008).

[34] C. Jäkel. "Numerisches Ausbreitungsmodell für Flüssigwasserstoff: Entwicklung, Validierung und sicherheitstechnische Anwendung in einer Verflüssigungsanlage im Rahmen eines Unfallszenarios". PhD thesis. RWTH Aachen, under review.